BULLETIN OF THE POLISH ACADEMY OF SCIENCES
TECHNICAL SCIENCES, Vol. 68, No. 2, 2020
DOI: 10.24425/bpasts.2020.133116

MECHANICAL AND AERONAUTICAL ENGINEERING, THERMODYNAMICS

Darcy-Forchheimer 3D Williamson nanofluid flow with generalized Fourier and Fick's laws in a stratified medium

M. RAMZAN[1,2]*, H. GUL[1], and M. ZAHRI[3]

[1] Department of Computer Science, Bahria University, 44000, Islamabad, Pakistan
[2] Department of Mechanical Engineering, Sejong University, Seoul 143-747, Korea
[3] Department of Mathematics, MASEP Research Group, University of Sharjah, P.O. Box 27272, Sharjah 61174, UAE

Abstract. Mathematical analysis for 3D Williamson nanofluid flow past a bi-directional stretched surface in Darcy-Forchheimer permeable media constitutes the focus of this study. The novelty of the proposed model is augmented by the addition of thermal and solutal stratification with chemical species and variable thermal conductivity. Calculations of the suggested model are conducted via the renowned homotopy analysis method (HAM). The results obtained are validated by comparing them in a limiting form with an already published article. Excellent harmony is achieved in this regard. Graphical structures, depicting impacts of assorted arising parameters versus the profiles involved are also provided. It is noticed that the velocity profile is a dwindling function of the Williamson parameter and Hartmann number. It is also stated that the Cattaneo-Christov heat flux exhibits conventional Fourier and Fick's laws behavior when both coefficients of thermal and concentration relaxations are zero.

Key words: Generalized Fourier and Fick's laws, Darcy-Forchheimer porous medium, Thermal and solutal stratification, Williamson nanofluid.

1. Introduction

The study of heat transfer is mandatory whenever there is a change in temperature between the boundaries or among the parts of a similar body. The heat transfer process has various applications in the industry and engineering, which include energy production, transfer of heat in tissues, pasteurization process of food, fuel cells and cooling atomic reactors, etc. Fourier [1] devised a law that provided the most effective model and has been the yardstick for many years because of its multiple applications. But, as a result of some drawbacks, this model often leads to an equation of parabolic energy, which specifies that in the beginning trouble was instantly met by the medium under attention. Cattaneo [2] addressed the irregularity in Fourier's law named "Paradox in heat conduction" by inserting the relaxation time. It was noted that this alteration results in hyperbolic energy equation. Eventually he made it possible for the heat to be transported in the form of thermal waves with limited speed. Nowadays, this updated model is termed the Cattaneo-Christov (CC) heat flux model. Hayat et al. [3] studied the effect of the CC heat flux model on Darcy-Forchheimer flow with constant density for third-grade liquid with varying thermal conductivity. Hashim and Khan [4] inspected the effect of the CC heat flux model on Carreau fluid flow near the stagnation point. Meanwhile, thin film nanofluid flow comprising nanotubes under the influence of CC heat flux is studied by Lu et al. [5]. The flow of third-grade fluid with CC heat flux accompanying homogeneous-heterogeneous (hh) reactions is studied by Ramzan et al. [6]. Vasu and Ray [7] numerically solved the Carreau nanofluid flow with CC heat flux. Lu et al. [8] numerically solved the mathematical model of nanofluid time-dependent flow containing both types of nanotubes between two rotating disks with hh reactions and the CC heat flux model. The flow generated by a rotating disk with CC heat flux is deliberated analytically by Imtiaz et al. [9]. The flow of Carreau fluid past a convectively heated stretched surface with variable thermal conductivity and CC heat flux is discussed by Lu et al. [10].

Nanofluids, an emerging field of engineering, has enthralled numerous researchers who were looking at ways to improve the efficiency of cooling processes in industry. This amalgamated fluid is unique in its own nature as nanofluids are prepared by means of implanting nanoparticles into base fluids. Significant improvement in thermal conductivity of the base fluid is witnessed through the addition of suspended metallic particles, and it constitutes a relatively new advancement in the engineering biosphere. Nanofluids possess interesting characteristics such as adequate viscosity, more stability, improved wetting, spreading, and dispersion features on the solid surface, even for fluids possessing weak nanoparticle concentrations [11]. The nanoparticles are usually composed of metals, non-metals, carbides and nitrides with comparatively high thermal conductivity. It is experimentally proved that up to 5% of nanoparticle volume fraction in nanofluids is quite enough for enhancement in effective heat transfer [12]. Diverse natural advantages of nanofluids may find their application in areas such as power generation, nuclear reactors, fuel

*e-mail: mramzan@bahria.edu.pk

Manuscript submitted 2019-08-14, revised 2019-12-04, initially accepted for publication 2019-12-20, published in April 2020

cells, transportation and biomedicine [13]. An important study on nanofluid flow has been reported by Ramzan et al. [14], using the series solution technique. Nasir et al. [15] studied the flow of nanofluid thin film comprising carbon nanotubes in a Darcy-Forchheimer porous medium. The flow of nanofluid with magnetohydrodynamics effects in a permeable medium through the Darcy-Forchheimer relation is scrutinized analytically by Rasool et al. [16]. Taseer et al. [17] used the optimum series scheme to investigate 3D nanofluid flow containing CNTs of both types in a Darcy-Forchheimer porous medium past a nonlinear stretched surface. Another exploration comprising nanofluid 3D flow with Darcy-Forchheimer expression as well as convective and hh reactions is solved optimally by Hayat et al. [18]. Farooq et al. [19] found an analytical solution of nanofluid flow between two squeezing parallel plates with melting heat transfer. Some more recent investigations highlighting various aspects of nanofluids may be found in [20–26] and many other publications.

Study of non-Newtonian fluids [27–29] plays a pivotal role in numerous engineering and industrial applications. Examples of non-Newtonian materials include blood, ketchup, different polymeric liquids, paints, jellies, soap, glues, gel and many more. When compared to viscous fluids, mathematical modeling of non-Newtonian fluids is very complex. Nevertheless, there have been numerous researchers that are contributing a lot on these fluids, highlighting their different features.

Stratification plays a pivotal role in many processes, either natural or industrial ones. This type of phenomenon evolves owing to the temperature and concentration variations of liquids with different densities. Various attempts and studies related to stratification have been made recently. Hamid et al. [30] discussed the flow of Williamson nanofluid past an expanding/contracting cylinder with a mixed convective double stratification medium. Khan et al. [31] numerically investigated the problem of Williamson nanofluid flow with thermal and solutal stratification, activation energy and entropy generation. The change in viscosity in Williamson nanofluid flow with both types of stratification is deliberated by Khan et al. [32]. An optimum series solution of 3D Williamson nanofluid flow with the convective boundary condition is found by Hayat et al. [33]. Many investigations on the significance of thermal stratification can be found in [34–36].

In view of the foregoing, it is revealed that abundant studies are available discussing 3D MHD Williamson nanofluid flows. But fewer deliberate the combined effects of chemical reaction and variable thermal conductivity. And no study so far has been conducted that deliberates the amalgamated impacts of generalized Fourier and Fick's laws with Darcy-Forchheimer expression and thermal & solutal stratifications. This is being tackled for the first time and will make a valuable contribution to the existing literature. Series solutions of the envisioned mathematical model are attained via the homotopy analysis method (HAM). Graphs of numerous parameters are also presented versus the distributions involved. To endorse the results given in the present exploration, a comparison table is provided, comparing those with an already published article in a limiting case, and excellent concurrence is recorded in this regard.

2. Mathematical modeling

Consider the 3D flow of a nanofluid over a bidirectional stretching surface with impacts of CC in a Darcy-Forchheimer porous medium. The fluid is flowing over the surface in x and y – directions with respective velocities $u = ax$ and $v = by$, respectively (Fig. 1). The analysis is performed in attendance of hh reactions and variable thermal conductivity.

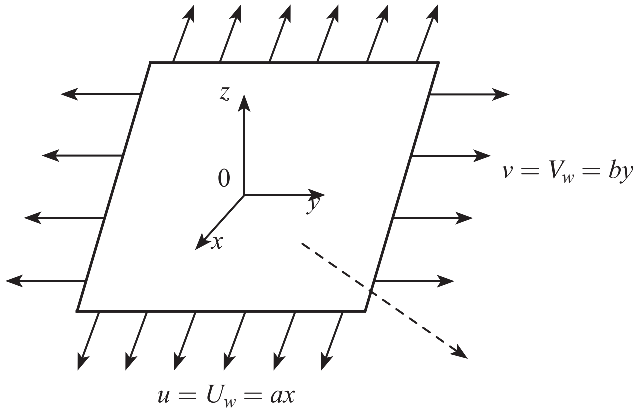

Fig. 1. Schematic diagram of the flow problem

By using the boundary layer approximation, the governing nonlinear PDEs are [37–38].

$$u_x + v_y + w_z = 0, \tag{1}$$

$$\begin{aligned} uu_x + vu_y + wu_z &= \upsilon u_{zz} + \sqrt{2}\upsilon\Gamma u_z u_{zz} - \\ &- \frac{\nu}{k^*}u - Fu^2 - \frac{\sigma B_0^2 u}{\rho}, \end{aligned} \tag{2}$$

$$\begin{aligned} uv_z + vv_y + wv_z &= \upsilon v_{zz} + \sqrt{2}\upsilon\Gamma v_z v_{zz} - \\ &- \frac{\nu}{k^*}v - Fv^2 - \frac{\sigma B_0^2 u}{\rho}, \end{aligned} \tag{3}$$

$$\begin{aligned} &uT_x + vT_y + wT_z + \lambda_E \phi_E = \\ &= \frac{1}{\rho c_p}\frac{\partial}{\partial z}(kT_z) + \tau\left[D_B C_z T_z + \frac{D_T}{T_\infty}(T_z)^2\right], \end{aligned} \tag{4}$$

$$\begin{aligned} &uC_x + vC_y + wC_z + \lambda_C \phi_C = \\ &= D_B C_{zz} + \frac{D_T}{T_\infty}T_{zz} - K_c(C - C_\infty), \end{aligned} \tag{5}$$

with $F = \frac{C_b}{xK^{1/2}}$ is the inertia coefficient.

$$\begin{aligned} \phi_E = {} & u^2 T_{xx} + v^2 T_{yy} + w^2 T_{zz} + 2uvT_{xy} + 2uwT_{xz} + \\ & + 2vwT_{yz} + (uu_x + vu_y + wu_z)T_x + \\ & + (uv_x + vv_y + wv_z)T_y + (uw_x + vw_y + ww_z)T_z, \end{aligned} \tag{6}$$

$$\phi_c = u^2C_{xx} + v^2C_{yy} + w^2C_{zz} + 2uvC_{xy} + 2uwC_{xz} + \\ + 2vwC_{yz} + (uu_x + vu_y + wu_z)C_x + \\ + (uv_x + vv_y + wv_z)C_y + (uw_x + vw_y + ww_z)C_z. \tag{7}$$

The subjected boundary conditions are
$u = U_w$, $v = V_w$, $w = 0$, $T = T_w = T_0 + A_1x$,
$C = C_w = C_0 + B_1x$, at $z = 0$

$$u \to 0,\ v \to 0,\ T \to T_\infty = T_0 + A_2x, \\ C \to C_\infty = C_0 + B_2x,\ \text{as}\ z \to \infty \tag{8}$$

using the following transformations:

$$u = axf'(\eta), \quad v = ayg'(\eta), \\ w = -\sqrt{av}\left(f(\eta) + g(\eta)\right), \quad \eta = \sqrt{\frac{a}{v}}z, \\ \theta(\eta) = \frac{T - T_\infty}{T_w - T_\infty}, \quad \phi(\eta) = \frac{C - C_\infty}{C_w - C_\infty}. \tag{9}$$

Considering thermal conductivity $k = k_a(1 + \varepsilon\theta(\eta))$, with $\varepsilon = (k_w - k_a)/k_a$, as given in [39–40]. The non-dimensional system of equation is given by:

$$f''' + Wef''f''' - f'^2 + ff'' + gf'' - \\ - \lambda_1 f' - Mf' - Frf'^2 = 0, \tag{10}$$

$$g''' + Weg''g''' - g'^2 + gg'' + fg'' - \\ - \lambda_1 g' - Mg' - Frg'^2 = 0, \tag{11}$$

$$(1 + \varepsilon\theta)\theta'' + \varepsilon\theta'^2 + \Pr N_b\theta'\phi' + \Pr N_t\theta'^2 - \\ - \Pr f'S - \Pr f'\theta + \Pr(f + g)\theta' - \\ - \delta_t \Pr\big((f + g)^2\theta'' - 2f'\theta'(f + g) + f'S + \\ + f'^2\,\theta - ff''S - ff''\theta - gf''S - gf''\theta + \\ + (f + g)(f' + g')\theta'\big) = 0, \tag{12}$$

$$\phi'' + \frac{N_t}{N_b}\theta'' + \Pr Le(f + g)\phi' + f'(P + \phi) - \\ - \Pr Le\delta_c\big((f + g)^2\phi'' - 2f'(f + g)\phi' + \\ + f'(P + \phi) + (f + g)(f' + g')\phi'\big) - k_c\phi = 0, \tag{13}$$

$$f(0) = 0, \quad f'(0) = 1, \quad g'(0) = \beta, \quad g(0) = 0, \\ \theta(0) = 1 - S, \quad \phi(0) = 1 - P, \quad f'(\infty) = 0, \\ g'(\infty) = 0, \quad \theta(\infty) = 0,\ 1\ \ \phi(\infty) = 0, \tag{14}$$

where

$$\Pr = \frac{\mu c_\rho}{k},\ N_t = \frac{\tau D_t(T_w - T_\infty)}{vT_\infty}, \\ N_B = \frac{\tau D_B(C_w - C_\infty)}{v},\ M = \frac{\sigma B_0^2}{\rho a},\ Le = \frac{\alpha}{D_B}, \\ P = \frac{B_2}{B_1},\ S = \frac{A_2}{A_1},\ \beta = \frac{b}{a},\ \delta_c = \lambda_c a,\ \delta_t = \lambda_E a, \\ Fr = \frac{C_b}{K^{\frac{1}{2}}},\ \lambda_1 = \frac{\upsilon}{k^* a},\ k = k_a\big(1 + \varepsilon\theta(\eta)\big), \\ \varepsilon = \frac{(k_w - k_a)}{k_a},\ We = \frac{\sqrt{2}a^{3/2}\Gamma x}{\sqrt{v}}. \tag{15}$$

Drag force coefficients C_{fx} and C_{fy} in the direction of x and y are given by:

$$C_{fx} = \frac{2\tau_{wx}}{\rho U_w^2},\ C_{fy} = \frac{\tau_{wy}}{\rho U_w^2}, \tag{16}$$

with

$$\tau_{wx}\big|_{z=0} = u_z = \frac{\Gamma}{\sqrt{2}}(u_z)^2, \tag{17}$$

$$\tau_{wy}\big|_{z=0} = v_z = \frac{\Gamma}{\sqrt{2}}(v_z)^2, \tag{18}$$

Dimensionless forms of drag force coefficients are:

$$C_{fx}\mathrm{Re}^{\frac{1}{2}} = \left[f'' + \frac{We}{2}(f'')^2\right]_{\eta=0}, \tag{19}$$

$$C_{fy}\mathrm{Re}^{\frac{1}{2}} = \left[g'' + \frac{We}{2}(g'')^2\right]_{\eta=0}, \tag{20}$$

where

$$\mathrm{Re}_x = \frac{U_w x}{v}. \tag{21}$$

3. Homotopic solutions

It was required to choose some appropriate technique that can address such a highly nonlinear mathematical problem. To address this issue homotopy analysis method (HAM) is applied to get an analytical solution in series form with associated boundary conditions. Earlier on researchers and scientists have looked for alternating analytical techniques owing to obvious limitations of the numerical schemes [41]. Amid these, perturbation methods prove most common and are being used extensively in theoretical and engineering problems [42].

But one major drawback of these methods, consisting in relying on small or large parameters and being effective only for weakly nonlinear problems, turns them into schemes with limited scope. Then non-perturbation schemes like the Adomian decomposition method [43], the δ – expansion method [44], the variational iteration method [45], and the Lyapunov's artificial small parameter [46] and so on are proposed to tackle this limitation of reliance on small/large parameters. But convergence of the solutions is not guaranteed in these schemes. These methods are only defined for weakly nonlinear mathematical models. However, the homotopy analysis method (HAM) claimed by Liao [41] addresses all highly nonlinear problems with sufficient choice to select parameters' values to warrant a convergent series solution. Contrary to numerical schemes, HAM can also tackle the far field boundary value problems. Salient characteristics of the said scheme are as follows:

1. HAM solutions are free from the selection of small/large parameters, unlike the perturbation schemes. Here, initial guess estimates are made to obtain the final solution based on the concept of homotopic deformation.
2. Convergence of the series solutions is controlled by the auxiliary parameter instead of the physical parameter.
3. HAM also provides us autonomy for the choice of initial guess estimates by keeping in view the physical system of the problem under consideration. This may be of polynomial, exponential, trigonometric or logarithmic nature. For example, for an oscillatory problem, a trigonometric function may be selected. For a problem with damping, the function may be of of $e^{-\eta}$ type.

The homotopy analysis method necessities initial guess estimates $(f_0, g_0, \theta_0, \phi_0)$ with auxiliary linear operators $(L_f, L_g, L_\theta, L_\phi)$ for the problem under consideration in the form given below:

$$f_0(\eta) = 1 - e^{-\eta}, \quad g_0(\eta) = \beta(1 - e^{-\eta}), \\ \theta_0(\eta) = (1 - S), \quad \phi_0(\eta) = (1 - P), \tag{22}$$

$$L_f = f''' - f', \quad L_g = g''' - g', \\ L_\theta = \theta'' - \theta', \quad L_\phi = \phi'' - \phi', \tag{23}$$

with

$$L_f[B_1 + B_2 + B_3] = 0, \quad L_g[B_4 + B_5 + B_6] = 0, \\ L_\theta[B_7 + B_8] = 0, \quad L_\phi[B_9 + B_{10}] = 0, \tag{24}$$

where $B_i (i = 1 - 7)$ symbolize arbitrary constants.

3.1 Analysis of convergence. Homotopy analysis method is applied to arrive at the solution in series form, and it also depends on auxiliary parameters. These auxiliary parameters are required to control the region of series solutions. For the present problem, the range of these parameters are:

$$-0.1 \le h_f \le -1.5, \quad -1.1 \le h_g \le -0.3, \\ -1.3 \le h_\theta \le -0.6, \quad -1.1 \le h_\phi \le -0.6.$$

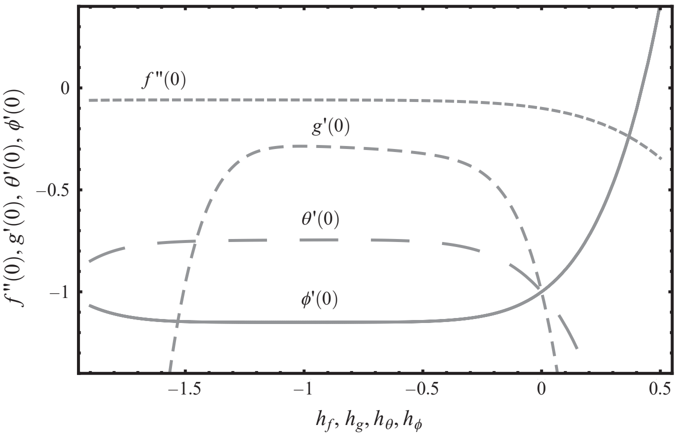

Fig. 2. h-curves for f, g, θ, ϕ

Table 1
Convergence for varied order of approximations of series solutions when
$\lambda_1 = 0.2$, $M = 0.4$, $Fr = 0.2$, $\beta = 0.1$, $N_b = 0.2$, $N_t = 0.8$, $\Pr = 0.7$, $\varepsilon = 0.1$, $Le = 1$, $\delta_c = \delta_t = 0.2$, $We = 1$, $n = 0.05$.

Order of approximation	$-f''(0)$	$-g''(0)$	$-\theta'(0)$	$-\phi'(0)$
01	1.0850	0.0797	0.4083	0.7773
05	1.1457	0.0760	0.2874	0.7446
10	1.1478	0.7589	0.2807	0.7443
15	1.1478	0.7589	0.2784	0.7425
20	1.1478	0.7589	0.2784	0.7429
25	1.1478	0.7589	0.2784	0.7429

Table 2
Comparison of $C_{fx}\mathrm{Re}^{1/2}$ with Nadeem et al. [47] for varied values of We in limiting case

We	$C_{fx}\mathrm{Re}^{1/2}$	**Present**
0.0	1	1
0.1	0.976588	0.976588
0.2	0.939817	0.939817
0.3	0.882720	0.882720

4. Results and discussion

This section is dedicated to examining the outcomes of evolving parameters on particular distributions. The response of Hartmann number M versus velocity components in x – and y – directions is represented in Fig. 3 and Fig. 4. It is witnessed that both velocity components are on the decline because of strong Lorentz force, which demonstrates resistance to the fluid's movement. The impact of the Williamson fluid parameter We on the velocity profile is presented in Fig. 5. It is seen that the velocity profile is a diminishing function of We. Physically, owing to higher values of relaxation time, increased fluid's

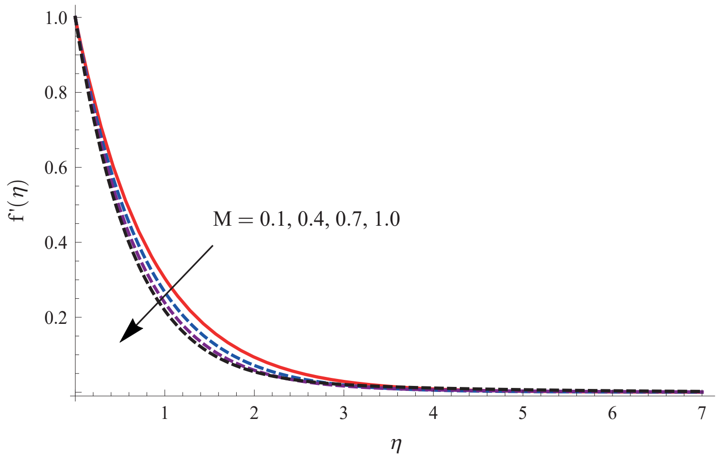

Fig. 3. Influence of M on f'

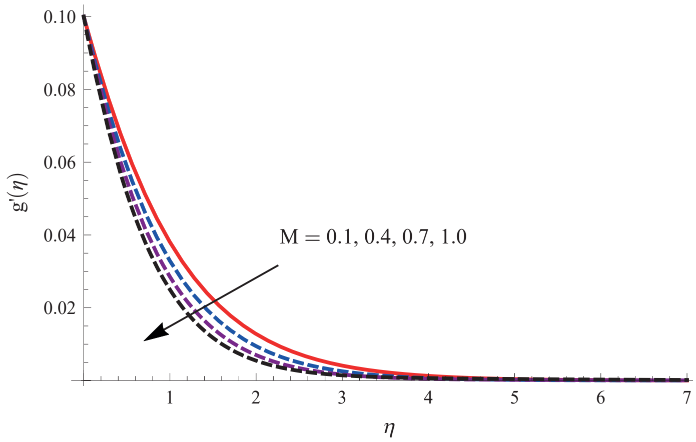

Fig. 4. Influence of M on g'

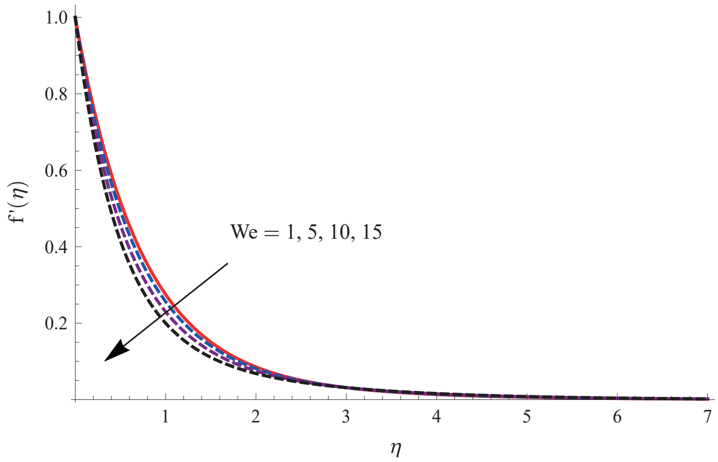

Fig. 5. Influence of We on f'

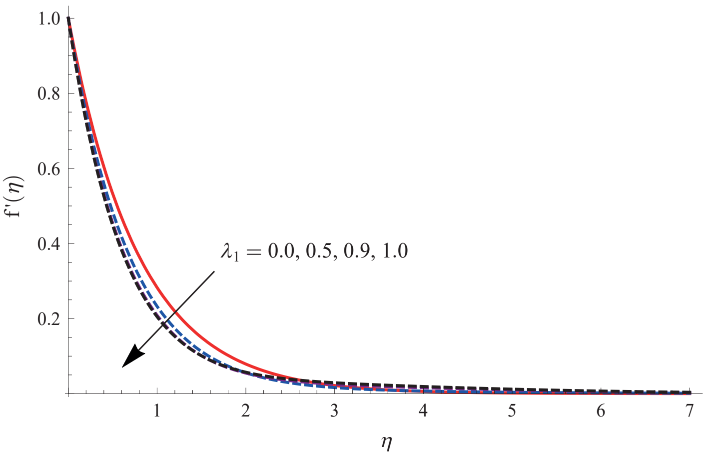

Fig. 6. Influence of λ_1 on f'

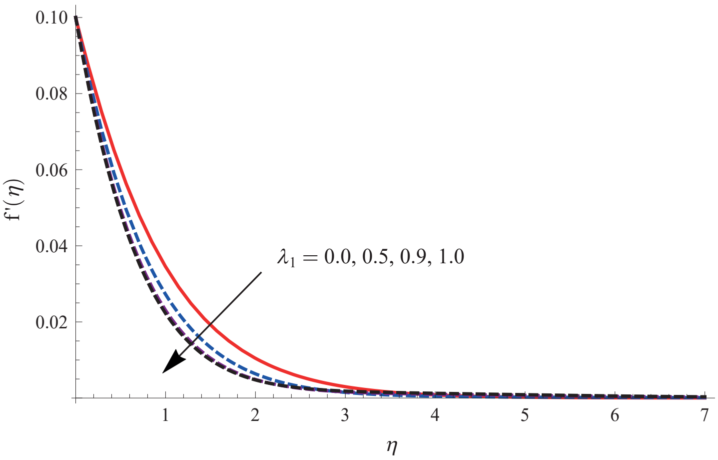

Fig. 7. Influence of λ_1 on g'

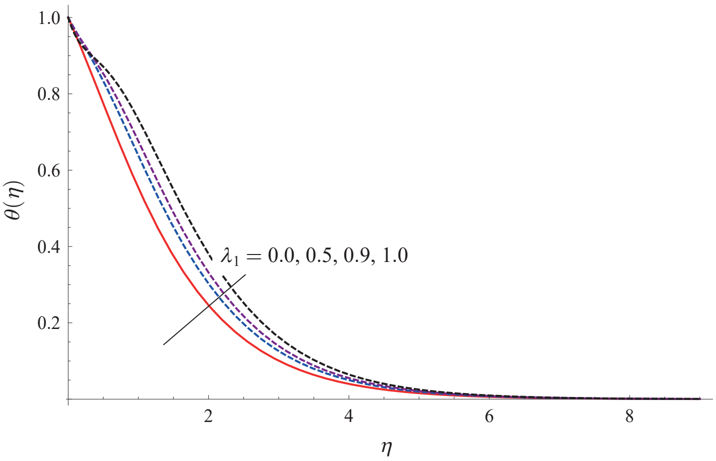

Fig. 8. Influence of ε on θ

resistance is seen. This ultimately results in decreased velocity of the fluid. Figures 6 and 7 are illustrated to witness the consequence of porosity parameter λ_1 on velocity profile components. It is seen that velocity is a declining function of λ_1 in both cases. Velocity of the fluid is on the decrease as the bottom surface of the fluid is more absorbent. Which is in fact a more realistic situation. Further, far-off from the surface, the impact of λ_1 is not very significant on the outer layer of the boundary layer and it does not affect fluid motion in this region. Figure 8 exemplifies the consequence of thermal conductivity parameter

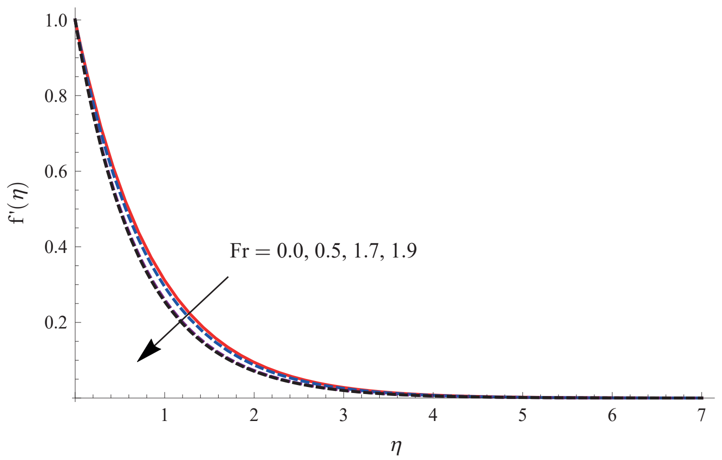

Fig. 9. Influence of Fr on f'

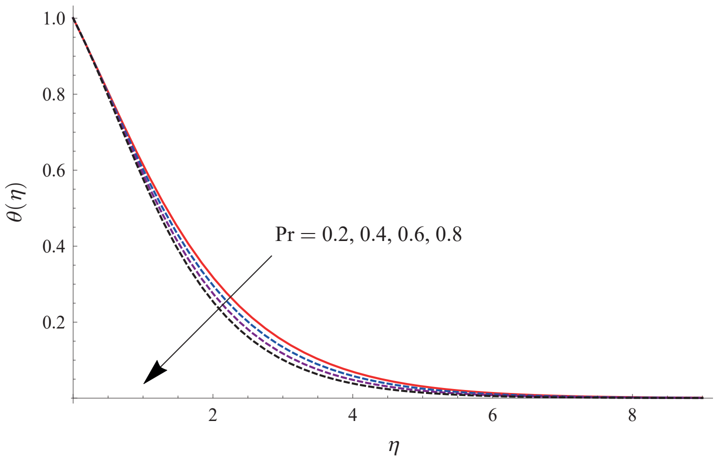

Fig. 10. Influence of Pr on θ

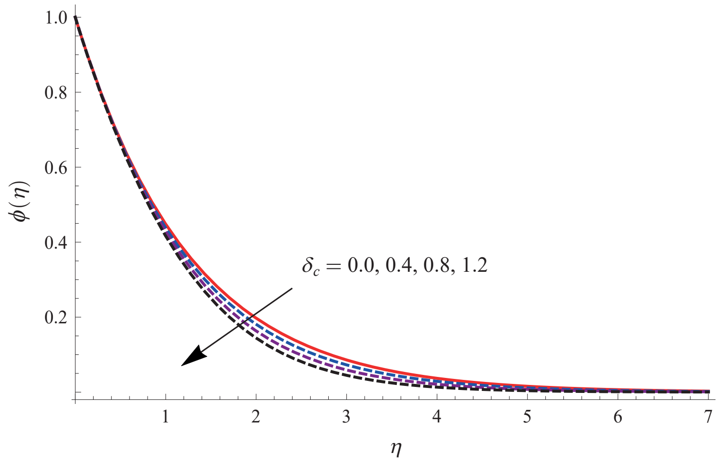

Fig. 11. Influence of δ_c on ϕ

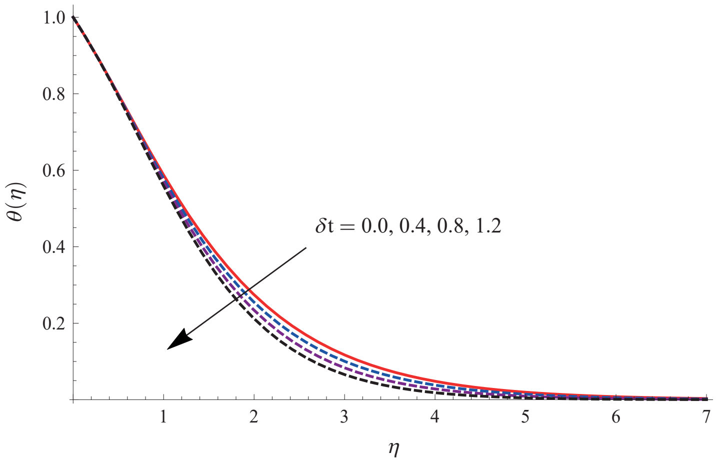

Fig. 12. Influence of δ_t on θ

ε on the temperature profile. The temperature of the fluid rises for larger values of ε. Thermal conductivity is defined as the rate of heat transfer via conduction. The larger the amount of heat transfer, the higher the temperature of the fluid. Figure 9 is drawn to see the impact of inertia coefficient Fr on the velocity profile. It is obvious from the figure that higher estimates of the Forchheimer number strengthen the resistance to fluid flow and as a result a decrease in velocity is observed. If $Fr = 0$ then the momentum boundary layer exhibits the Darcy's flow. The impact of Prandtl number Pr on temperature distribution is portrayed in Fig. 10. It is detected that the rate of heat transfer from the hot surface tends to slow down for larger estimates of Pr. That is why a decrease in temperature of the fluid is noticed. Figure 11 and Fig. 12 depict the effect of concentration and thermal relaxation times δ_c and δ_t on concentration and temperature distributions, respectively. From the figures, it is seen that both profiles are declining functions of respective relaxation times. In fact, higher estimates of relaxation times result in non-conductive behavior of the material which is responsible for a decrease in temperature and concentration fields. It is further seen that for $\delta_c = \delta_t = 0$ the CC heat flux acts according to conventional Fourier and Fick's laws. The influence of thermophoresis parameter Nt on concentration and temperature profiles is displayed in Fig. 13 and Fig. 14, respectively. Both concentration and temperature fields will increase owing to higher values of Nt. Actually, for higher values of Nt,

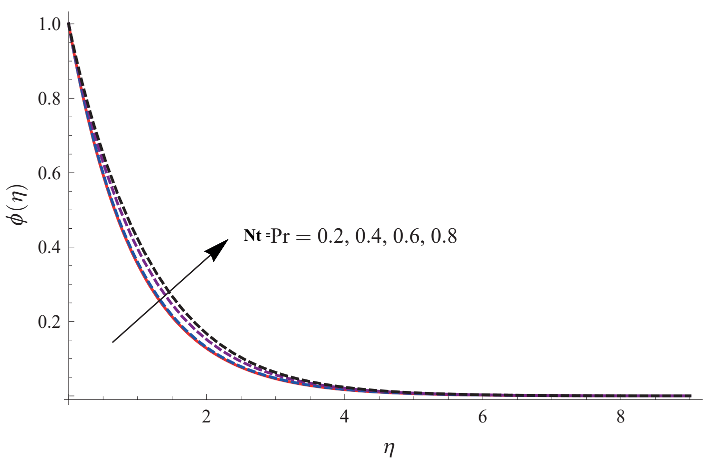

Fig. 13. Influence of N_t on ϕ

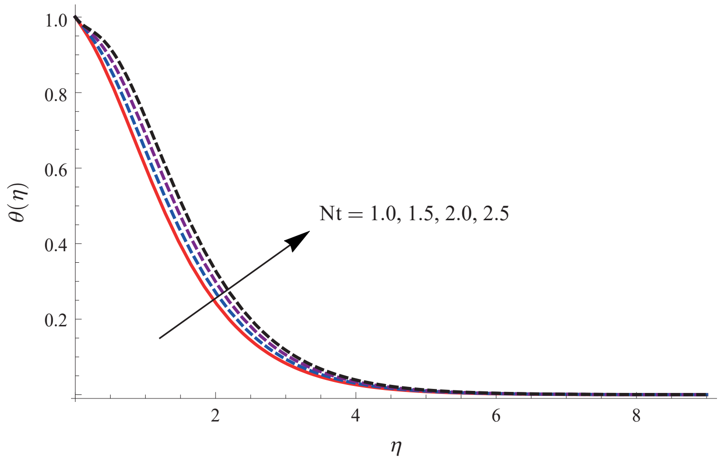

Fig. 14. Influence of N_t on θ

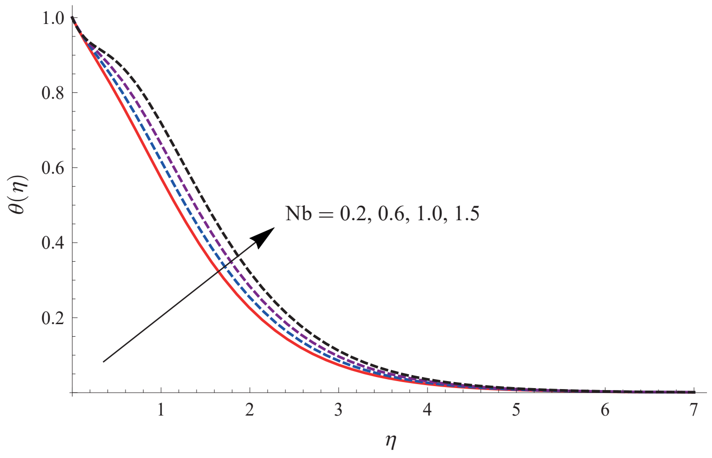

Fig. 15. Influence of N_b on θ

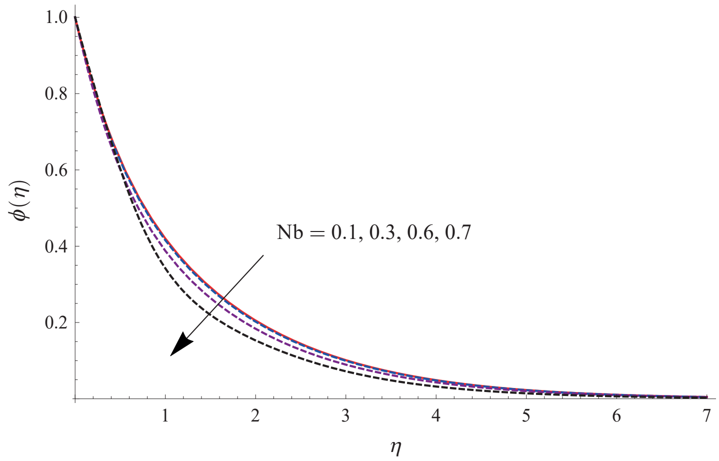

Fig. 16. Influence of N_b on ϕ

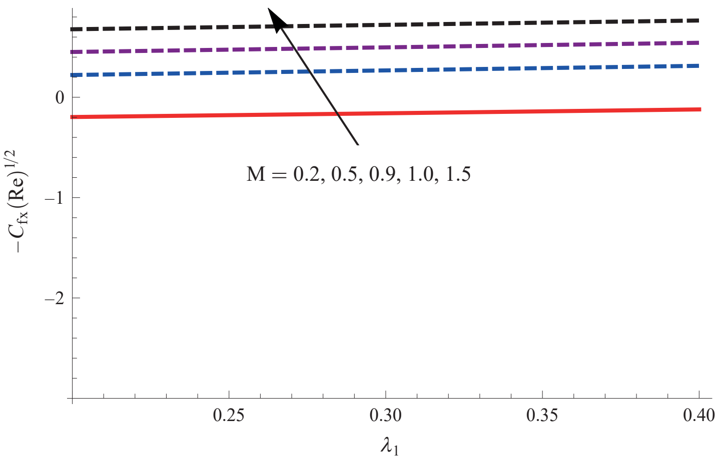

Fig. 17. Influence of λ_1 and M on Drag force

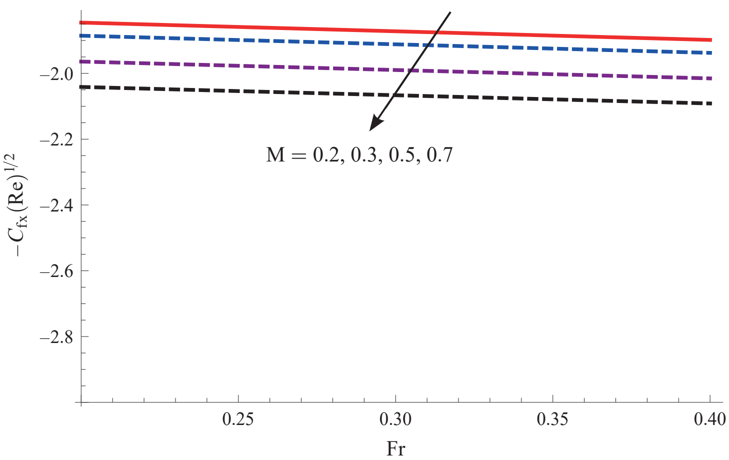

Fig. 18. Influence of M and Fr on Drag force

the temperature of the fluid far away from the surface will be boosted due to the transfer of nanoparticles. Thus, augmented profiles are observed in both cases. The impact of Brownian motion parameters N_b on temperature and concentration profiles is presented in Figs. 15 and 16. Larger estimates of Nt escalate the temperature of the fluid but also reduce concentration. Figure 17 is used to present the effects of local porosity number λ_1 and Hartmann number M. It is gathered that the drag force coefficient is a growing function of both parameters λ_1 and M. It is a known fact that increase in λ_1 will slow the fluid flow and thus strengthen the friction force. Similarly, higher values of M also assist the Lorentz force that hampers the movement of the fluid's flow. Thus, increased estimates of fluid drag force are observed. Similar behavior is seen for the values of M and Fr. This effect is shown in Fig. 18.

5. Final remarks

Analytical solutions for three-dimensional MHD Williamson nanofluid flow with variable thermal conductivity and generalized Fourier and Fick's laws over a bidirectional stretched surface are found. Double stratification conditions are utilized to solve the problem. Results are obtained using HAM. Significant results of the present problem are summarized as follows:

- The velocity profile is a diminishing function of the Williamson parameter and Hartmann number.
- The fluid's temperature rises for larger estimates of the thermal conductivity parameter.
- For both thermal relaxation times $\delta_c = \delta_t = 0$, the Cattaneo-Christov heat flux illustrates conventional Fourier and Fick's laws.
- Opposite behavior is noticed for the thermophoresis parameter and Brownian motion parameter versus nanoparticle concentration distribution.
- The drag force coefficient is augmented with increased values of M, λ_1 and Fr.

Conflicts of interest. The authors declare no conflict of interest.

Acknowledgements. This work is supported by the University of Sharjah (UOS), MASEP Research Group, RGS-2018–2019 and Research Project No. 1802144069.

References

[1] J. Fourier and B.J. La, "Théorie analytique de la chaleur", *Mem. Acad. R. Sci.* 8, 581–622 (1829).

[2] C. Cattaneo, "Sulla conduzione del calore", *Atti Sem. Mat. Fis. Univ. Modena.* 3, 83–101 (1948).

[3] T. Hayat, M. Ijaz Khan, S.A. Shehzad, M. Imran Khan, and A. Alsaedi, "Numerical simulation of Darcy-Forchheimer flow of third grade liquid with Cattaneo-Christov heat flux model", *Math Method Appl Sci.* 41(12), 4352–4359 (2018).

[4] M. Khan, "On Cattaneo-Christov heat flux model for Carreau fluid flow over a slendering sheet", *Results. Phys.* 7, 310–319 (2017).

[5] D. Lu, M. Ramzan, M. Mohammad, F. Howari, and J.D. Chung, "A thin film flow of nanofluid comprising carbon nanotubes influenced by Cattaneo-Christov heat flux and Entropy generation", *Coatings*, 9(5), 296 (2019).

[6] M. Ramzan, M. Bilal, and J.D. Chung, "Effects of MHD homogeneous-heterogeneous reactions on third grade fluid flow with Cattaneo-Christov heat flux", *J. Mol. Liq.* 223, 1284–1290 (2016).

[7] B. Vasu and A.K. Ray, "Numerical study of Carreau nanofluid flow past vertical plate with the Cattaneo-Christov heat flux model", *Int. J. Numer. Method. H.* 29(2), 702–723 (2019).

[8] D. Lu, Z. Li, M. Ramzan, A. Shafee, and J. D. Chung, "Unsteady squeezing carbon nanotubes based nano-liquid flow with Cattaneo-Christov heat flux and homogeneous–heterogeneous reactions", *Appl. Nanosci.* 9(2), 169–178 (2019).

[9] M. Imtiaz, A. Kiran, T. Hayat, and A. Alsaedi, "Axisymmetric flow by a rotating disk with Cattaneo-Christov heat flux", *J. Braz. Soc. Mech. Sci. & Eng.* 41(3), 149 (2019).

[10] D. Lu, M. Mohammad, M. Ramzan, M. Bilal, F. Howari, and M. Suleman, "MHD boundary layer flow of Carreau fluid over a convectively heated bidirectional sheet with non-Fourier heat flux and variable thermal conductivity", *Symmetry*. 11(5), 618 (2019).

[11] S. Shateyi and J. Prakash, "A new numerical approach for MHD laminar boundary layer flow and heat transfer of nanofluids over a moving surface in the presence of thermal radiation", *Bound Value Probl*. 2014(1), 2 (2014).

[12] K. Khanafer, K. Vafai, and M. Lightstone, "Buoyancy-driven heat transfer enhancement in a two-dimensional enclosure utilizing nanofluids", *Int J Heat Mass Tran.* 46(19), 3639–3653 (2003).

[13] K.V. Wong and O. De Leon, "Applications of nanofluids: current and future", *Adv Mech Eng*. 2, 519659 (2010).

[14] M. Ramzan, M. Sheikholeslami, M. Saeed, and J.D. Chung, "On the convective heat and zero nanoparticle mass flux conditions in the flow of 3D MHD Couple Stress nanofluid over an exponentially stretched surface", *Sci Rep*. 9(1), 562 (2019).

[15] S. Nasir, Z. Shah, S. Islam, E. Bonyah, and T. Gul, "Darcy-Forchheimer nanofluid thin film flow of SWCNTs and heat transfer analysis over an unsteady stretching sheet", *AIP Adv.* 9(1), 015223 (2019).

[16] G. Rasool, A. Shafiq, C. M. Khalique, and T. Zhang, "Magneto-hydrodynamic Darcy-Forchheimer nanofluid flow over nonlinear stretching sheet", *Phys. Scripta..* (2019).

[17] T. Muhammad, D.C. Lu, B. Mahanthesh, M.R. Eid, M. Ramzan, and A. Dar, "Significance of Darcy-Forchheimer porous medium in nanofluid through carbon nanotubes", *Commun. Theor. Phys.* 70(3), 361 (2018).

[18] T. Hayat, A. Aziz, T. Muhammad, and A. Alsaedi, "An optimal analysis for Darcy-Forchheimer 3D flow of nanofluid with convective condition and homogeneous–heterogeneous reactions", *Phys. Lett. A.* 382(39), 2846–2855 (2018).

[19] M. Farooq, S. Ahmad, M. Javed, and A. Anjum, "Melting heat transfer in squeezed nanofluid flow through Darcy Forchheimer medium", *J. Heat. Transf.* 141(1), 012402 (2019).

[20] S. Rashidi, S. Akar, M. Bovand, and R. Ellahi, "Volume of fluid model to simulate the nanofluid flow and entropy generation in a single slope solar still", *Renew Energ.* 115, 400–410 (2018).

[21] R. Ellahi, A. Zeeshan, N. Shehzad, and S.Z. Alamri, "Structural impact of Kerosene-Al2O3 nanoliquid on MHD Poiseuille flow with variable thermal conductivity: application of cooling process", *J. Mol. Liq.* 264, 607–615 (2018).

[22] M. Hassan, M. Marin, R. Ellahi, and S.Z. Alamri, "Exploration of convective heat transfer and flow characteristics synthesis by Cu–Ag/water hybrid-nanofluids", *Heat Transf Res.* 49(18), 1837–1848 (2018).

[23] M. Hassan, M. Marin, A. Alsharif, and R. Ellahi, "Convective heat transfer flow of nanofluid in a porous medium over wavy surface", *Phys. Lett. A.* 382(38), 2749–2753 (2018).

[24] N. Shehzad, A. Zeeshan, R. Ellahi, and S. Rashidi, "Modelling study on internal energy loss due to entropy generation for non-darcy poiseuille flow of silver-water nanofluid: an application of purification", *Entropy* 20(11), 851 (2018).

[25] M. Hassan, R. Ellahi, M. M. Bhatti, and A. Zeeshan, "A comparative study on magnetic and non-magnetic particles in nanofluid propagating over a wedge", *Can. J. Phys.* 97(3), 277–285 (2018).

[26] A. Sohail, M. Fatima, R. Ellahi, and K.B. Akram, "A videographic assessment of Ferrofluid during magnetic drug targeting: an application of artificial intelligence in nanomedicine", *J. Mol. Liq.* 285, 47–57 (2019).

[27] R. Ellahi, "The effects of MHD and temperature dependent viscosity on the flow of non-Newtonian nanofluid in a pipe: analytical solutions" , *Appl. Math. Model.* 37(3), 1451–1467 (2013).

[28] M. A. Yousif, H.F. Ismael, T. Abbas, and R. Ellahi, "Numerical study of momentum and heat transfer of MHD Carreau nanofluid over an exponentially stretched plate with internal heat source/sink and radiation", *Heat. Transf. Res.* 50(7) (2019).

[29] R. Ellahi, S. M. Sait, N. Shehzad, and N. Mobin, "Numerical simulation and mathematical modeling of electro-osmotic Couette-Poiseuille flow of MHD Power-law nanofluid with Entropy generation", *Symmetry* 11(8), 1038 (2019).

[30] A. Hamid, M. Alghamdi, M. Khan, and A.S. Alshomrani, "An investigation of thermal and solutal stratification effects on mixed convection flow and heat transfer of Williamson nanofluid", *J. Mol. Liq*, 284, 307–315 (2019).

[31] M. Khan, S. Qayyum, T.A. Khan, M.I. Khan, T. Hayat, I. Ullah, and A. Alsaedi, "Optimization of thermal and solutal stratification in simulation of Williamson fluid with entropy generation and activation energy", *Heat. Transf. Res.* 50(9(2019)).

[32] M. Khan, T .Salahuddin, M.Y. Malik, and F.O. Mallawi, "Change in viscosity of Williamson nanofluid flow due to thermal and solutal stratification"; *Int. J. Heat. Mass. Tran.* 126, 941–948 (2018).

[33] T. Hayat, M.Z. Kiyani, A. Alsaedi, M.I. Khan, and I. Ahmad, "Mixed convective three-dimensional flow of Williamson nanofluid subject to chemical reaction", *Int. J. Heat. Mass. Trans.* 127, 422–429(2018) (2018).

[34] M. Ramzan, M. Bilal, and J.D. Chung, "Effects of thermal and solutal stratification on Jeffrey magneto-nanofluid along an inclined stretching cylinder with thermal radiation and heat generation/absorption", *Int J Mech Sci.* 131, 317–324 (2017).

[35] M. Ramzan, N. Ullah, J.D. Chung, D. Lu, and U. Farooq, "Buoyancy effects on the radiative magneto Micropolar nanofluid flow with double stratification, activation energy and binary chemical reaction", *Sci Rep.* 7(1), 12901 (2017).

[36] M. Ramzan, M. Bilal, and J.D. Chung, "Radiative flow of Powell-Eyring magneto-nanofluid over a stretching cylinder with chemical reaction and double stratification near a stagnation point", *PloS one.* 12(1), e0170790 (2017).

[37] M. Ramzan, M. Bilal, J.D. Chung, D.C. Lu, and U. Farooq, "Impact of generalized Fourier's and Fick's laws on MHD 3D second grade nanofluid flow with variable thermal conductivity and convective heat and mass conditions", *Phys Fluids.* 29(9), 093102 (2017).

[38] T. Hayat, A. Aziz, T. Muhammad, and A. Alsaedi, "Darcy-Forchheimer three-dimensional flow of Williamson nanofluid over a convectively heated nonlinear stretching surface", *Commun. Theor. Phys.* 68(3), 387 (2017).

[39] H. Zargartalebi, M. Ghalambaz, A. Noghrehabadi, and A. Chamkha, "Stagnation-point heat transfer of nanofluids toward stretching sheets with variable thermo-physical properties", *Adv. Powder. Technol.* 26(3), 819–829 (2015).

[40] F.M. Abbasi and S.A. Shehzad, "Heat transfer analysis for three-dimensional flow of Maxwell fluid with temperature dependent thermal conductivity: Application of Cattaneo-Christov heat flux model", *J. Mol. Liq.* 220, 848–854 (2016).

[41] S. Liao, "Beyond perturbation: Introduction to the Homotopy Analysis method", *Chapman and Hall/CRC* (2003).

[42] P.J. Message, "Perturbation Theory: Techniques and Limitations. From Newton to Chaos: Modern Techniques for Understanding and Coping with Chaos in N-Body Dynamical Systems", pp. 5–19 (1995).

[43] G. Adomian, "A review of the decomposition method in applied mathematics", *Electron J Math Anal Appl,* 135(2), 501–544 (1988).

[44] J. Awrejcewicz, I.V. Andrianov, and L.I. Manevitch, "Asymptotic approaches in nonlinear dynamics", *New trends and applications* (Vol. 69). Springer Science & Business Media (2012).

[45] J.H. He, "Variational iteration method–a kind of non-linear analytical technique: some examples", *Int. J. Nonlinear. Mech*. 34(4), 699–708 (1999).

[46] A.M. Lyapunov, "The general problem of the stability of motion", *Int. J Control*. 55 (3), 531–534 (1992).

[47] S. Nadeem, S. T. Hussain, and C. Lee, "Flow of a Williamson fluid over a stretching sheet", *Brazilian J. Chem. Eng.* 30(3), 619–625 (2013).